Spatial–temporal analysis of land cover dynamics in the Southern Aral Sea region using remote sensing and GIS (2004–2024)

Yunus Karimov[1, *], *Iroda* Orifjonova[1], *Ruza* Ballieva[2], *Keunimjay* Allanazarov[2], *Nurlan* Khudayberganov[2], and *Shohista* Abdurozokova[3]

[1]Samarkand State Pedagogical Institute, 140044 Samarkand, Uzbekistan
[2]Karakalpak State University, 230100 Nukus, Uzbekistan
[3]Samarkand State University, 230100 Samarkand, Uzbekistan

Abstract. The Southern Aral Sea region has undergone profound environmental transformations over the past several decades due to severe reduction of inflowing water and intensified evaporation processes. The purpose of this study is to use remote sensing and GIS tools to examine the spatiotemporal changes in land cover in the Southern Aral Sea region during the past 20 years. Changes in important land cover types, such as water bodies, vegetation, mudflats, pure sand, and sandy salt surfaces, were evaluated using multi-temporal Landsat ETM+ and Landsat 8 OLI satellite photos obtained between 2004 and 2024. A hybrid method based on the Normalized Difference Vegetation Index (NDVI) and the Soil-Adjusted Vegetation Index (SAVI) was used to classify land cover. The findings show that the lake's surface area has significantly decreased while saline and sandy land cover has rapidly expanded, creating and intensifying the Aral-Kum Desert. Water-covered regions significantly decreased annually, according to quantitative study, whereas saline and sandy surfaces increased proportionately. Strong correlations between land cover change, lake shrinkage, and important climate variables, especially wind speed and air temperature, are shown using correlation analysis. These results demonstrate how important land cover dynamics are in hastening the creation of dust storms and desertification processes in the Southern Aral Sea region. In dry areas, the used remote sensing and GIS-based method supports sustainable land and ecosystem management and offers an efficient framework for long-term environmental monitoring.

1 Introduction

The Aral Sea crisis is widely regarded as one of the most severe anthropogenic environmental transformations in arid Central Asia. The degradation of the lake system was primarily caused by the long-term diversion of the Amu Darya and Syr Darya rivers for irrigated agriculture, which sharply reduced the volume of water reaching the terminal basin. Whereas the historical annual inflow to the Aral Sea was approximately 56 km³, it declined to nearly 5

* Corresponding author: Yunus.karimov01@gmail.com

km³ in some periods, and in particularly dry years river discharge did not reach the lake at all [1]. This hydrological imbalance intensified evaporation from the shallow lake surface and initiated a rapid process of desiccation, shoreline retreat, and ecosystem destabilization [2].

The consequences of this transformation extend far beyond the reduction of water surface area. As the lake retreated, vast areas of the former seabed became exposed to atmospheric processes. These surfaces gradually developed into the Aral-Kum Desert, a newly formed anthropogenic desert composed of unconsolidated sandy, saline, and silty sediments. The exposed seabed is highly vulnerable to aeolian erosion and has become an important source of salt-dust emissions in the region [3]. Wind-driven transport of fine particles contributes to the redistribution of salts, minerals, and potentially toxic elements over long distances, affecting soils, agricultural lands, settlements, and human health [4]. Therefore, the spatial expansion of sandy and saline surfaces is not only a geomorphological process but also a major ecological and socio-economic risk factor.

Dust and sand storms originating from the Aral-Kum Desert are closely connected with land cover degradation. Bare sandy and saline surfaces provide easily mobilized material, while high wind speed and increasing air temperature strengthen evaporation, soil drying, and particle transport. During aeolian movement, dust particles interact with the atmosphere, hydrosphere, and terrestrial ecosystems, influencing sediment composition and biogeochemical cycles [5]. The intensity and frequency of these processes make continuous monitoring essential, especially in densely populated areas located near the former shoreline.

Previous studies have examined long-term changes in the Aral Sea using hydrological observations, satellite imagery, geospatial modelling, and environmental risk assessment. These studies have shown substantial differences between the Northern and Southern Aral Sea basins. Since the mid-1980s, the lake has been divided into separate water bodies. The Northern Aral Sea has demonstrated partial recovery due to water regulation measures, whereas the Southern Aral Sea has continued to shrink and fragment [6, 7]. At the same time, land cover changes in the exposed seabed remain highly dynamic and require detailed spatial assessment over extended time intervals.

Remote sensing and geographic information systems provide an effective methodological framework for studying such transformations. Satellite observations make it possible to detect changes in water bodies, vegetation, mudflats, sandy surfaces, and saline deposits over large territories with consistent spatial and temporal coverage. In arid and semi-arid regions, index-based approaches are especially useful because they allow researchers to distinguish vegetation cover from bare soil and to assess the progression of desertification. The Normalized Difference Vegetation Index (NDVI) is widely applied to identify photosynthetically active vegetation, while the Soil-Adjusted Vegetation Index (SAVI) improves interpretation in landscapes where sparse vegetation and exposed soil dominate [8–10].

The Southern Aral Sea region represents a particularly important case for multitemporal land cover analysis. Its location within the Turan Lowland, combined with arid climatic conditions, limited water availability, and intensive wind activity, creates favorable conditions for desertification. As water-covered areas decline, sandy and saline surfaces expand, increasing the environmental pressure on surrounding territories. Although numerous studies have addressed the general shrinkage of the Aral Sea, further investigation is needed to quantify the relationship between water loss, land cover transformation, and climatic factors over the last two decades.

This study aims to assess spatiotemporal land cover dynamics in the Southern Aral Sea region during 2004–2024 using Landsat satellite imagery, GIS tools, and index-based classification. The research focuses on five major land cover classes: water bodies, mud/swamp areas, vegetation, pure sand, and sandy salt surfaces. The objectives are to quantify changes in these classes, estimate the average annual water shrinkage rate, and determine statistical relationships between land cover dynamics and climatic variables, particularly wind speed and average seasonal air temperature. The results contribute to a better understanding of desertification processes, dust storm formation, and long-term environmental degradation in the Southern Aral Sea region.

2 Materials and methods

The study was designed as a multitemporal remote sensing and GIS-based assessment of land cover dynamics in the Southern Aral Sea region for the period 2004–2024. The analysis relied on Landsat satellite imagery obtained from the open Earth Explorer and Glovis repositories. Cloud-free scenes acquired at the end of the year were selected to ensure seasonal comparability and to minimize the influence of short-term vegetation variability. Landsat ETM+ 7 and Landsat 8 OLI data were used because of their long observation record, 16-day revisit interval, and 30 m spatial resolution, which is sufficient for regional-scale monitoring of water shrinkage and desert surface expansion [9]

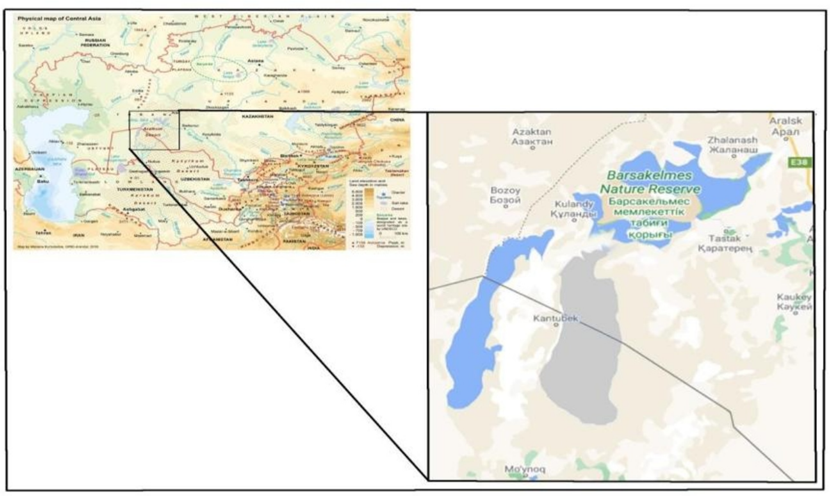

Fig. 1. Location of the Aral Sea (Source: GRID-Arendal).

The historical boundary of the Aral Sea was reconstructed using the Physical Map of Central Asia from 1960, where the lake area was approximately 68,000 km². This map was digitized and integrated into the GIS environment to provide a reference layer for comparing historical and contemporary land cover patterns. The main processing and spatial analysis procedures were performed in ArcGIS. Before classification, all satellite images underwent preprocessing, including atmospheric correction, geometric correction, image mosaicking, clipping to the study area, and removal of boundary distortions. To optimize processing time and improve visualization, the images were resampled to a 150 m × 150 m grid. Land cover classification was carried out using a combined index-based approach. First, the Normalized Difference Vegetation Index (NDVI) was calculated to identify photosynthetically active vegetation. NDVI values range from −1 to +1 and were derived using the near-infrared and red spectral bands of the Landsat sensors. Areas with NDVI values above 0.3 were interpreted as vegetation cover and excluded from subsequent bare-surface classification. Second, the Soil-Adjusted Vegetation Index (SAVI) was applied to improve the discrimination of sparsely vegetated, sandy, saline, and exposed soil surfaces. The soil adjustment coefficient was set at L = 0.5 following Huete's approach. The final land cover maps were produced by combining NDVI- and SAVI-based classifications.

Five major land cover classes were identified: water bodies, mud/swamp areas, vegetation, pure sand, and sandy salt surfaces. The classified maps were reclassified in ArcGIS to obtain quantitative estimates of each class area. The average annual water shrinkage rate was calculated by comparing changes in water-covered area across the study period. Statistical analysis was performed in R. Correlation analysis was used to examine relationships among land cover classes, while additional correlation tests assessed the association between water shrinkage, sandy surface expansion, wind speed, and average seasonal air temperature. Statistical significance was evaluated at the $p < 0.05$ level. The methodology follows the logic of long-term remote sensing monitoring applied to dryland degradation and desertification studies [10–12].

3 Results and discussion

The drying of the Aral Sea during the last 20 years has substantially transformed the landscape of the former seabed. As a result, the newly formed Aral-Kum Desert has expanded across the exposed area (Fig. 2). The land cover map illustrates the main spatial changes observed in the study area during the analyzed period.

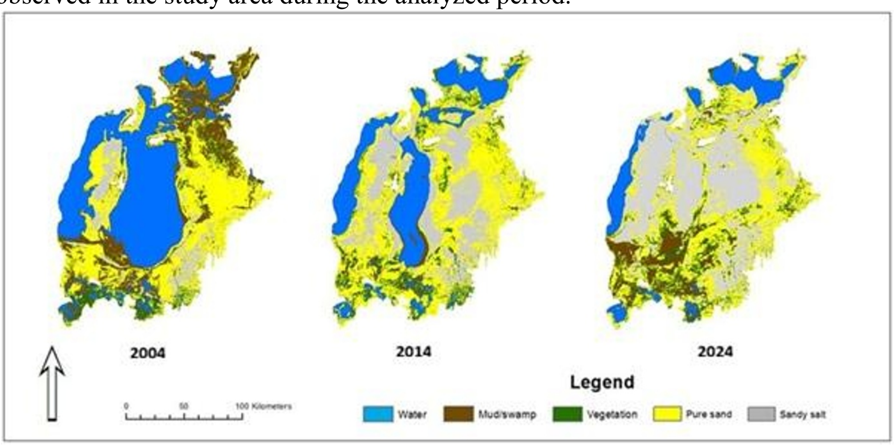

Fig. 2. Dynamics of land-cover change in the Aral Sea from 2004 to 2024.

The land cover maps derived from the combined NDVI and SAVI classification demonstrate a pronounced reduction in the lake surface area. At the same time, sandy and saline sandy surfaces expanded significantly, particularly toward the eastern and central parts of the former seabed. The spatial distribution of these classes indicates that saline sand initially increased in the eastern sector and later migrated toward the central zone under the influence of natural processes. Mudflats and vegetation-covered areas were less affected by the expansion of hazardous sandy and saline surfaces. To quantify the distribution of land cover classes, the “Reclassify” operation in ArcGIS was used to convert qualitative land cover maps into quantitative spatial data. The results are presented in Fig. 3.

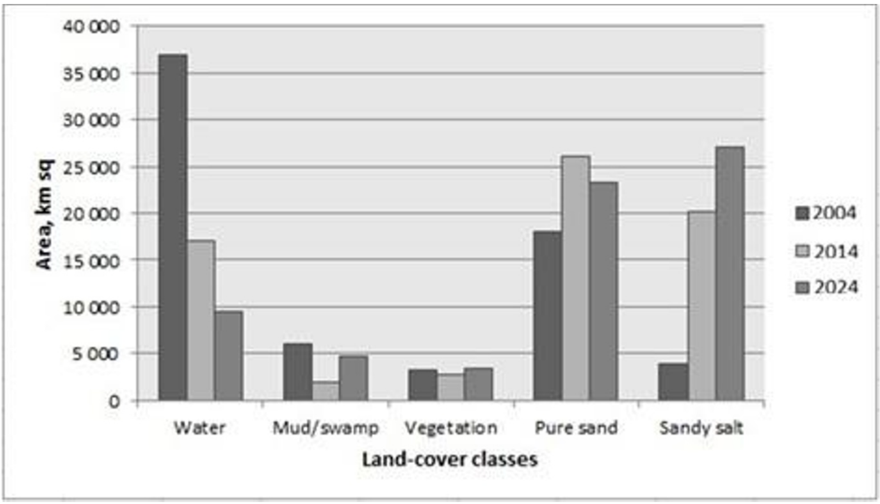

Fig. 3. Dynamic of land cover classes from 2004 to 2024.

Figure 3 shows a clear increase in pure sand and sandy salt areas, despite some interannual fluctuations. In 2004, sandy surfaces occupied approximately 18,000 km², while sandy salt areas covered less than 5,000 km². By 2024, pure sand and sandy salt classes had expanded by approximately 5,000 km² and 20,000 km², respectively. During the same period, the lake surface decreased by approximately 25,000 km². Mud and vegetation classes remained relatively stable throughout the analysis period, with vegetation showing greater spatial stability than mud-covered areas. Based on the total increase and decrease in land cover classes, the average annual water shrinkage rate was estimated at 1,372.65 km² per year. After estimating the shrinkage rate, correlation analysis was conducted to determine the relationships between water and other land cover classes. The results are presented in Table 1.

Table 1. Correlation analysis of land cover classes.

The correlation matrix shows that water area is positively correlated with mud/swamp areas (0.66) and vegetation (0.59). This suggests that larger lake surface areas are associated with the preservation of moist and vegetated land cover types. Conversely, water area is strongly and negatively correlated with pure sand and sandy salt surfaces, with correlation coefficients of −0.99 for both classes. This indicates that lake shrinkage is directly associated with the expansion of exposed sandy and saline surfaces. To assess whether the observed dynamics of water shrinkage were statistically significant, ANOVA was applied to the water area data. The analysis produced an R^2 value of 0.83 across three observations. The calculated F ratio was 3.532, while the F critical value was 3.478. The p-value was used to evaluate statistical significance, where $p > 0.05$ indicates insignificance and $p < 0.05$ indicates significance. The results are shown in Table 2.).

 https://doi.org/10.1051/e3sconf/202671907001

Table 2. ANOVA output.

Variation source	Sum of squares	Degrees of freedom	Mean square	F statistic	p-value	Critical F value
Intergroup variation	1.04E+09	4	2.59E+08	3.532	0.0028	3.478
Intragroup variation	7.34E+08	10	7.34E+07	—	—	—
Total variation	1.77E+09	14	—	—	—	—

After identifying the relationships among land cover classes, additional correlation analysis was conducted to examine the association between major land cover types and climatic variables. Water, pure sand, and sandy salt were compared with average summer air temperature and wind speed recorded at two meteorological stations near the study area.

Table 3. Correlation coefficients between climate factors and land-cover classes.

‘Aralskoe More’ meteo-station				
‘Uyaly’ meteostation				

The results in Table 3 indicate a strong relationship between climatic factors and lake shrinkage. Average seasonal air temperature and wind speed are negatively correlated with water area, confirming their role in accelerating evaporation and desiccation. At both meteorological stations, higher temperatures and stronger winds correspond to reduced lake surface area. The same climatic variables are positively correlated with pure sand and sandy salt surfaces. This relationship is especially important because these land cover types consist of fine and mobile particles that can be transported by wind. Therefore, the expansion of sandy and saline surfaces, combined with increasing wind activity and high temperatures, strengthens the risk of dust and sand storm formation. The correlation results suggest that climatic factors affect the Southern Aral Sea ecosystem primarily through their influence on water loss and the subsequent exposure of erodible sediments. These findings indicate the need to revise and strengthen regional climate adaptation and land management policies.

4 Conclusions

The analysis demonstrates that the drying of the Southern Aral Sea between 2004 and 2024 caused a substantial transformation of land cover in the former seabed. The most important result is the formation and expansion of the Aral-Kum Desert, which now occupies a large area previously covered by water. As the lake surface declined, sandy and saline sandy surfaces expanded rapidly, while mud and vegetation classes remained comparatively stable. The average annual water shrinkage rate was estimated at 1,372.65 km^2. Correlation analysis confirmed a strong negative relationship between water area and both pure sand and sandy salt classes. This indicates that the reduction of lake surface directly contributes to the expansion of exposed desert surfaces. Climatic factors, especially wind speed and average summer air temperature, were strongly associated with both water loss and the growth of mobile sandy and saline surfaces.

The formation of the Aral-Kum Desert increases the risk of dust and sand storms because exposed sediments contain dry fine particles, salts, and potentially harmful substances. Although most Aral-Kum sediments show low concentrations of heavy metals, local geological and anthropogenic factors may still influence the spatial distribution of pollutants. High variability in dust deposition, particle size, and chemical composition confirms the need for continuous field monitoring in densely populated areas of the Southern Aral Sea region. The applied remote sensing and GIS-based approach provides a cost-effective and reproducible framework for long-term monitoring of land cover dynamics in arid regions. Such monitoring is necessary for assessing desertification, understanding dust transport processes, evaluating risks to human health and land use, and supporting sustainable regional environmental management.

References

1. R. Bazarbayev, B. Zhou, A. Allaniyazov, G. Zeng, D. Mamedov, E. Ivanitskaya, Q. Wei, H. Qian, K. Yakubov, M. Ghali, S. Karazhanov, Physical and chemical properties of dust in the Pre-Aral region of Uzbekistan, Environ. Sci. Pollut. Res. (2022).
2. H. He, R. Hamdi, G. Luo, P. Cai, M. Zhang, H. Shi, C. Li, P. Termonia, P. De Maeyer, A. Kurban, Numerical study on the climatic effect of the Aral Sea, Atmos. Res. 105977 (2021).
3. Q. Wu, H. Yue, Y. Liu, E. Hou, Geospatial quantitative analysis of the Aral Sea Shoreline changes using RS and GIS techniques, Earth Sci. Informatics **2** (2021).
4. F. Löw, D. Dimov, S. Kenjabaev, S. Zaitov, G. Stulina, V. Dukhovny, Land cover change detection in the Aralkum with multi-source satellite datasets, GIScience Remote Sens., 1–19 (2021).
5. J. Wang, D. Liu, J. Ma, Y. Cheng, L. Wang, Development of a large-scale remote sensing ecological index in arid areas and its application in the Aral Sea Basin, J. Arid Land **13**, 40–55 (2021).
6. W. Liu, L. Ma, J. Abuduwaili, Historical change and ecological risk of potentially toxic elements in the lake sediments from north Aral sea, central Asia, Appl. Sci. **10** (2020).
7. M. Alexyuk, A. Bogoyavlenskiy, P. Alexyuk, Y. Moldakhanov, V. Berezin, I. Digel, Epipelagic microbiome of the Small Aral Sea: Metagenomic structure and ecological diversity, Microbiologyopen **10** (2021).
8. F. Löw, A. V. Prishchepov, F. Waldner, O. Dubovyk, A. Akramkhanov, C. Biradar, J. P. A. Lamers, Mapping Cropland abandonment in the Aral Sea Basin with MODIS time series, Remote Sens. **10** (2018).
9. Y. Su, D. Wang, S. Zhao, J. Shi, Y. Shi, D. Wei, Examining long-term natural vegetation dynamics in the Aral Sea Basin applying the linear spectral mixture model, PeerJ **9**, e10747 (2021).
10. X. Pan, W. Wang, T. Liu, Y. Huang, P. De Maeyer, C. Guo, Y. Ling, S. Akmalov, Quantitative detection and attribution of groundwater level variations in the amu darya delta, Water (Switzerland) **12**, 1–20 (2020).
11. A. Khaitbaev et al., Anthropogenic transformation of oasis landscapes in Khorezm Province, Uzbekistan: A geoecological analysis, E3S Web of Conferences **497**, 02043 (2024).
12. A. Massakbayeva, J. Abuduwaili, S. Bissenbayeva, B. Issina, Z. Smanov, Water balance of the Small Aral Sea, Environ. Earth Sci. **79**, 1–11 (2020).